

MEASUREMENT AND CORRELATION OF SOLUBILITY OF DISPERSE ANTHRAQUINONE AND AZO DYES IN SUPERCRITICAL CARBON DIOXIDE

Seung Nam Joung, Hun Yong Shin, Young Hwan Park* and Ki-Pung Yoo[†]

Department of Chemical Engineering, Sogang University, C.P.O. Box 1142, Seoul, Korea

*KITECH, San 17-1, HongChonRi, IJangMyun, ChonAnSi, 330-820, Korea

(Received 19 August 1997 • accepted 4 November 1997)

Abstract – The solubility of three disperse anthraquinone dyes and two azo dyes in supercritical CO₂ was measured. The tested dyes are Celliton fast blue B, 1-amino-2-methylantraquinone, 1-methylaminoanthraquinone, disperse Red 1 and 4-[4-(phenylazo)phenylazo]-o-cresol. Solubility measurements were made at 313.15-393.15 K and 10-25 MPa in a high-temperature autoclave phase equilibrium apparatus. Pure physical properties of the dyes such as critical constants, molar volumes and vapor pressures were estimated based on semi-empirical methods. Also, the data were quantitatively modeled by both an empirical density correlation and a quantitative equation of state recently proposed by the present authors based on nonrandom lattice theory. We found that anthraquinone disperse dyes in general show higher solubility than azo disperse dyes in supercritical CO₂ within the experimental ranges.

Key words: Experimental Method, Solubility of Disperse Anthraquinone and Azo Dyes, Supercritical Carbon Dioxide, Density Correlation, Equation of State Lattice Theory

INTRODUCTION

The structure of synthetic PET fibers is in general crystalline with homogeneous micropores. Thus, to color them, low molecular weight disperse dyes have been used to date. Conventional wet dyeing processes for coloring synthetic PET-structured fibers with disperse dyes create several environmental problems such as utilizing excess amounts of water and discharging toxic chemical additives. Thus, to mitigate such water pollution problems related to the wet dyeing process, attention has been placed in recent years on the development of new dyeing technologies. One noteworthy idea involves the implementation of so-called supercritical fluid dyeing (SFD) technology [Gerbert et al., 1994; Saus et al., 1993; Knittel et al., 1993].

In SFD, a dyeing agent is dissolved into supercritical gaseous solvent and dyeing proceeds in a gaseous atmosphere rather than in an aqueous liquid phase. Especially if nonpolar carbon dioxide is used as a dyeing medium in the SFD, the medium shows a favorable physical affinity with hydrophobic disperse dyeing agents. As a result, gas-phase SFD can be realized even without adding chemical additives in a dyeing process. Thus, the dyeing can be done at a supercritical state of dye in a relatively short time [Chiou et al., 1985; Fleming and Koros, 1986; Swidersky et al., 1994].

However, necessary thermophysical property data and phase equilibrium information of systems containing disperse dyes in supercritical fluids have been extremely limited to date since SFD is an emerging dyeing technology. Although limited ex-

perimental information such as the solubility of dyes in supercritical fluids is available [Chang et al., 1996], no reliable study of phase equilibrium modeling is available because of the complex chemical structure of the dye compounds. For example, even pure physical properties of dyes such as critical constants, molar volume and vapor pressure at the standard state are not available.

Thus, in the present study, we performed systematic thermodynamic modeling of the supercritical fluid phase equilibrium of systems containing dye species in supercritical carbon dioxide. In doing so, we emphasized experimental measurement of solubility, empirical estimation of pure physical properties based on literature [Lyman et al., 1990; Reid et al., 1987, etc.], and finally the modeling solubility behavior of dye species in supercritical carbon dioxide based on a new empirical density correlation model [Bartle et al., 1991; Özcan et al., 1997] and a quantitative prediction by an equation of state (EOS).

Recent success of the NLF (Nonrandom Lattice Fluid) EOS formulated by one of the present authors [You et al., 1994a, b, c] encouraged us to extend the model to complex systems such as dye compounds in supercritical fluids. We report here the quantitative modeling results of phase equilibrium of dyes in supercritical carbon dioxide.

EXPERIMENTAL

1. Reagents

Sample dye compounds, e.g., disperse Blue 14 (commercial name, Celliton fast blue B, 97.9%), disperse Orange 11 (1-amino-2-methylantraquinone, 95%), 1-methyl-aminoanthraquinone(98%), disperse Red 1(95%), and disperse Yellow 7(4-

[†]To whom all correspondence should be addressed.
E-mail: kpyoo@ccs.sogang.ac.kr

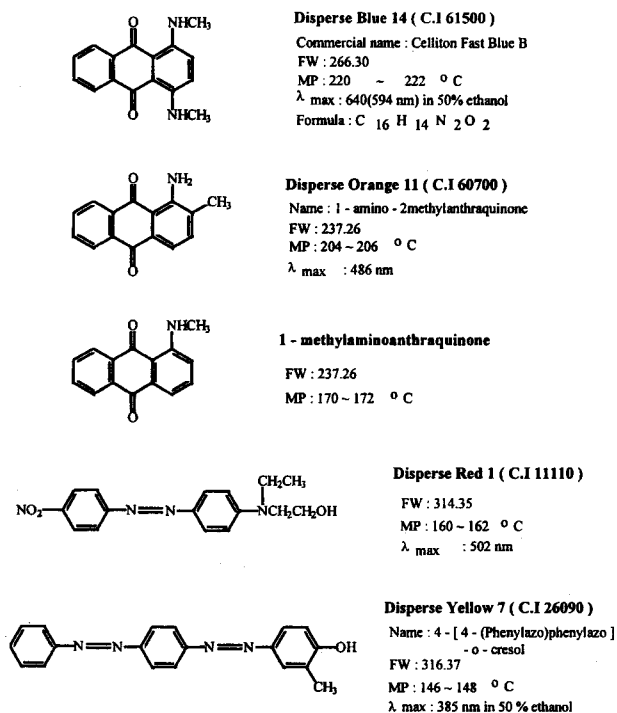


Fig. 1. Chemical structures of tested disperse dyes.

[4-(phenylazo)phenylazo]-o-cresol, 95%) were purchased from Aldrich Co. (<95%, USA). The chemical structure of the dye samples is shown in Fig. 1. CO₂ (<99.9%) was purchased from Seoul Gas Co. (Seoul, Korea).

2. Experimental Apparatus

An autoclave-type phase equilibrium apparatus was used and the schematic diagram is shown in Fig. 2. The internal volume of the cell was 60 ml made with stainless steel 316. The cell was immersed in a heating mantle and the apparatus can operate safely up to 473.15 K and 40 MPa. To minimize pressure disturbances, a reservoir tank (1 L) was installed in front of the preheater. Pressure at the cell was maintained by a gas booster (HASKEL 75/15, USA) and the pressure was measured by a Heise pressure gauge (HEISE MM-43776, USA). The equilibrium temperature was controlled by a PID controller (DX9, Hanyoung Co., Korea). The tempera-

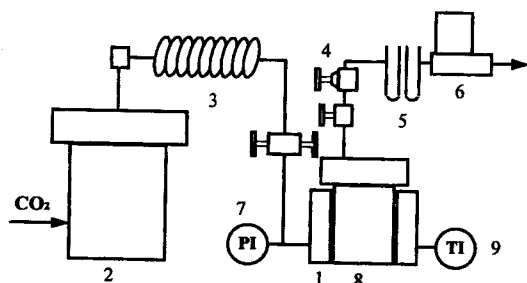


Fig. 2. Schematic diagram of supercritical fluid dyeing apparatus.

- | | | |
|-------------------|-----------------------|---------------------|
| 1: Heating mantle | 5: Cold trap | 8: Equilibrium cell |
| 2: Reservoir | 6: Mass flow meter | 9: Temperature |
| 3: Preheater | 7: Pressure indicator | indicator |
| 4: Metering valve | | |

ture was controlled to within ± 1 K range and the pressure was controlled to within ± 0.5 MPa.

The flow of CO₂ was preheated before entering the cell. The temperature was measured at the inlet, the outlet and inside the cell. The flow rate of effluent from the cell was controlled by a metering valve in the range of 200-300 ml/min, and the amount of equilibrated effluent from the cell was measured by a mass flow meter (TESCOM, USA). The equilibrated effluent was passed through the two-step acetone trap where the dissolved sample dye was separated from CO₂. After each experimental run, the whole line of the apparatus was rinsed by methanol, chloroform, and acetone, respectively, and dried. The residual solvents in the separated solute were completely removed by a rotary vacuum evaporator. For each sample solute, the experiment was repeated three times.

3. Spectroscopic Analysis

Since each sample dye has a coloring pattern and unique maximum frequency, λ_{\max} , the amount of each solute was analyzed by a UV-visible recording spectrophotometer (UV-240, Shimadzu, Japan). The calibration curve for each solute was constructed within an error range of $\pm 0.5\%$ and used for measuring the solubility.

THERMODYNAMIC MODELING

1. Estimation of Physical Properties of Pure Dyes

Information of physical constants for pure substances is essential for modeling the phase equilibrium of mixtures by a quantitative thermodynamic model such as EOS. However, for disperse dyes like most other molecularly complex substances, almost no information of pure physical constants was reported in literature. Thus, the pure physical properties necessary for the phase equilibrium modeling of mixtures containing dye substances have to be based on a type of estimation method. We employed existing group contribution methods to estimate the necessary physical properties [Lyman et al., 1990]. From this reference, Lyderson-Forman-Thodos's method for boiling point (T_b) and critical temperature (T_c), Miller's method for critical pressure (P_c), critical volume (V_c), critical compressibility factor (Z_c) and acentric factor (ω) were used. Also, the molar volumes and vapor pressures were estimated by Bhirud's method and Lee-Kestler's correlation, respectively [Reid et al., 1987]. The estimated pure property constants for dyes tested in the present study are summarized in Table 1. These properties in Table 1 are used for the estimation of parameters in the EOS employed in a later section.

2. Empirical Correlation of Solubility

An empirical method can be used to make a crude correlation of measured solubility data. The experimental solubility data obtained in the present study were illustratively correlated by a recent simple empirical equation [Bartle et al., 1991; Özcan et al., 1997]. The model equation is given in Eq. (1),

$$\ln\left(\frac{y_2 p}{p_{ref}}\right) = A + c(\rho - \rho_{ref}) \quad (1)$$

where y_2 is the mole fraction solubility, p is the pressure, A and c are constants, p_{ref} is a standard pressure of 1 bar, ρ is

Table 1. Estimated pure physical properties of disperse dyes

	Tc (K)	Pc (bar)	Vc (cm ³ /mol)	ω	Solid volume (cm ³ /mol)
Disperse blue 14	949.49	24.59	762	0.6702	202.29
Disperse orange 11	922.87	28.38	661	0.5811	177.86
1-Methylamino- anthraquinone	910.62	27.62	671	0.5778	177.86
Disperse red 1	929.11	19.07	922	0.7918	238.92
Disperse yellow 7	930.21	20.04	926	0.6381	245.42

Table 2. Best-fit parameters of Eq. (3) for the calculation of solubility of dye/CO₂ systems

Name	a	b/K ⁻¹	c/kgm ⁻³
Disperse blue 14	17.368	-8461.71	0.01085
Disperse orange 11	17.216	-7903.93	0.01202
1-Methylamino- anthraquinone	19.054	-8298.45	0.01025
Disperse red 1	23.328	-10552.6	0.01207
Disperse yellow 7	19.892	-9073.40	0.01246

the density of the solution, and ρ_{ref} is a reference density for which a value of 700 kgm⁻³ was used for calculations. The reason for using ρ_{ref} is to make the value of A much less sensitive to experimental error in the data and to avoid the large variations caused by extrapolation to zero density. A is given by

$$A = a + b/T \quad (2)$$

where T is the absolute temperature. Combining Eqs. (1) and (2), the empirical model equation becomes

$$\ln\left(\frac{y_2P}{P_{ref}}\right) = a + \frac{b}{T} + c(\rho - \rho_{ref}) \quad (3)$$

From the experimental data, each isotherm was fitted using Eq. (1) to obtain values A and c. The values c were then averaged for each dye, and the values given in Table 2 were obtained. Then, the isotherms were refitted to obtain new values of A using the averaged values of c. These values were plotted against 1/T for each dye, and values a and b were obtained from Eq. (2), which are also given in Table 2.

3. Modeling Phase Equilibria by NLF EOS

For a quick correlation of the solubility data, an empirical thermodynamic model, i.e., Eq. (3), can be a convenient tool. However one cannot apply the model for the purpose of extrapolated application of the measured data. Thus, for SFD process design, it is not a reliable tool and a further quantitative EOS must be used. Thus, we attempted to apply a theoretical EOS for the phase equilibrium of dyes in supercritical carbon dioxide.

Since the NLF-EOS, which was recently proposed by one of the present authors [You et al., 1994a, b, c], may not be familiar to some readers, we briefly present here the essential expressions of the model. Omitting details, the pressure-explicit NLF-EOS for a general mixture is given by

$$P = \frac{1}{\beta V_H} \left\{ \frac{z}{2} \ln \left[1 + \left(\frac{q_M}{r_M} - 1 \right) \rho \right] - \ln(1 - \rho) \right\} - \left(\frac{z}{2} \right) \theta^2 \left(\frac{\epsilon_M}{V_H} \right) \quad (4)$$

where ϵ_M is defined as,

$$\epsilon_M = \frac{1}{\theta^2} \left\{ \sum \sum \theta_i \theta_j \epsilon_{ij} + \left(\frac{\beta}{2} \right) \sum \sum \sum \theta_i \theta_j \theta_k \epsilon_{ijk} \right. \\ \left. (\epsilon_{ij} + 3\epsilon_{ki} - 2\epsilon_{jk}) \right\} \quad (5)$$

Summations are over all molecular species unless otherwise specified. In Eqs. (4) and (5), $\beta=1/kT$, $\theta_i=N_iq_i/N_q$, $q_M=\sum x_i q_i$, $r_M=\sum x_i r_i$, $\rho_i=N_i x_i/N_r$, $\rho=\sum \rho_i$ and x_i is the mole fraction of species i. ϵ_{ij} is the absolute value of the interaction energy between a segment of species i and that of species j, which is assumed to be,

$$\epsilon_{ij} = (\epsilon_{ii} \epsilon_{jj})^{1/2} [1 - (\lambda_{ij}^{(0)} T + \lambda_{ij}^{(1)})] \quad (6)$$

where $\lambda_{ij}(T)$ is the temperature-dependent binary interaction parameter, and the cross interaction energy ϵ_{ij} between holes and molecular species is assumed to be zero. The coefficients $\lambda_{12}^{(0)}$ and $\lambda_{12}^{(1)}$ were fitted by the experimental solubility data obtained in the present study.

Other expressions such as the chemical potential essential for phase equilibrium calculations will be omitted here [You et al., 1994a, b, c].

If in Eqs. (4) and (5), the subscripts i and j are simply let go to 1, the EOS reduced to EOS for a pure system. It is

$$P = \left(\frac{1}{V_H \beta} \right) \left\{ \left(\frac{z}{2} \right) \ln \left[1 + \left(\frac{q_1}{r_1} - 1 \right) \rho \right] - \ln(1 - \rho) \right\} \\ - \left(\frac{z}{2} \right) \theta_1^2 \left(\frac{\epsilon_M}{V_H} \right) \quad (7)$$

where

$$\rho = r_1 N_1 / N_r \quad (8)$$

$$V_1 = r_1 N_A V_H \quad (9)$$

$$\epsilon_M = \epsilon_{11} \left[1 - \left(\frac{\beta \epsilon_{11}}{2} \right) \theta_0 (2\theta_1 - \theta_0) \right] \quad (10)$$

In the derivation of Eqs. (4)-(10), the general relation $zq_1=zr_1-2r_1+2$ is employed. Therefore the characteristic volume given by Eq. (9) gives sufficient information for determining r_1 and q_1 . The other molecular parameter is ϵ_{11} . As in previous work [You et al., 1994a], we set $z=10$ and $V_H=9.75$ cm³mol⁻¹. Thus for real pure fluids we only need to determine two independent molecular parameters, r_1 (or V_1) and ϵ_{11} from two independent property data at a system temperature. These two parameters determined by a regression analysis of pure physical properties (e.g., molar density and vapor pressure, etc.) at each

Table 3. Estimated values of coefficients in NLF EOS parameters defined by Eqs. (11) and (12)

	E _a	E _b	E _c	V _a	V _b	V _c
Disperse blue 14	65.6948	0.2360	0.1106	97.8674	-0.0666	-0.4886
Disperse orange 11	70.9300	0.2577	0.2000	76.1657	-0.0485	-0.5135
1-Methylamino-anthraquinone	70.6337	0.2547	0.2090	77.2306	-0.0486	-0.5802
Disperse red 1	63.5591	0.2281	0.1110	110.8961	-0.0779	-0.5988
Disperse yellow 7	63.2136	0.2223	0.0937	113.3635	-0.0560	-0.5240

isotherm were fitted to the following empirical correlations as a function of temperature for convenient use in engineering practice.

$$\varepsilon_{1f}/k = E_a + E_b(T - T_0) + E_c \left(T \ln \frac{T_0}{T} + T - T_0 \right) \quad (11)$$

$$V_1^* = V_a + V_b(T - T_0) + V_c \left(T \ln \frac{T_0}{T} + T - T_0 \right) \quad (12)$$

where the reference temperature T_0 is set by 298.15 K. Values of the coefficients in Eqs. (11) and (12) for pure dyes and carbon dioxide used in the present study were determined from pure property data given by Table 1 and other data reported in the literature [Timmermans, 1950]. They are summarized in Table 3.

RESULTS AND DISCUSSION

1. Experimental Solubility Data

The measured solubility in mole fraction (y_2) of each sample dye in supercritical CO₂ at 313.15, 353.15 and 393.15 K and 10, 15, 20, and 25 MPa, respectively, is summarized

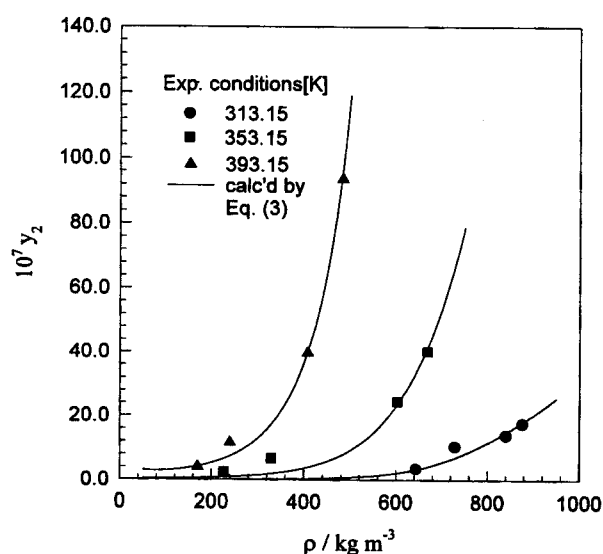
Table 4. Measured mole fraction solubility, y_2 , of disperse dyes in supercritical carbon dioxide

Name	P/MPa	$10^7 y_2$		
		T/K=313.15	353.15	393.15
Disperse blue 14	10	2.599	2.439	4.006
	15	12.868	10.067	12.850
	20	10.649	24.419	39.644
	25	14.493	40.240	93.490
Disperse orange 11	10	7.491	4.258	7.712
	15	38.451	24.571	51.403
	20	71.769	127.655	141.446
	25	74.938	182.143	270.687
1-Methylamino-anthraquinone	10	11.575	20.487	89.637
	15	56.100	59.539	144.702
	20	106.596	295.934	501.252
	25	129.281	382.138	707.403
Disperse red 1	10	0.651	0.811	2.111
	15	4.288	3.226	8.667
	20	8.178	16.345	42.745
	25	9.869	49.981	147.232
Disperse yellow 7	10	3.275	2.681	3.795
	15	18.998	14.355	16.766
	20	28.191	55.315	78.385
	25	31.342	86.943	184.756

in Table 4. According to the data, the solubility in general was increasing with increasing temperature and pressure of CO₂. Also, the low molecular weight anthraquinone dyes (i.e., disperse orange, blue and 1-methylaminoanthraquinone) show higher solubility than the azo dyes (i.e., disperse red and yellow) at any fixed condition. Among anthraquinone dyes, the low molecular weight dyes (i.e., disperse orange and 1-methylaminoanthraquinone) were more soluble than the disperse blue. Since we could not find similar data so far in literature, we did not compare the data obtained in this work with other data sources. Instead, we performed measurements at least three times for each temperature and pressure to support the reliability of the data.

2. Empirical Solubility Correlation

Using the best-fitted parameters in Eqs. (1) and (3), Figs. 3 and 4 show the correlated solubility of disperse blue 14 and disperse red 1 in supercritical carbon dioxide. In these figures, experimental data were compared together. Agreement between the correlated and experimental values for both dyes is good. Therefore, the model can be used to calculate the solubility of dyes in supercritical fluid at any equilibrium condition [Bartle et al., 1991; Özcan et al., 1997]. This type of empirical correlation may not be used for reliable extrapolation outside the experimental conditions. However, it is simple and useful for evaluating the effect of equilibrium conditions on the solubility. We omit further graphical illustrations for other cases.

**Fig. 3. Empirical solubility correlation by Eq. (3) for disperse blue 14 in supercritical CO₂.**

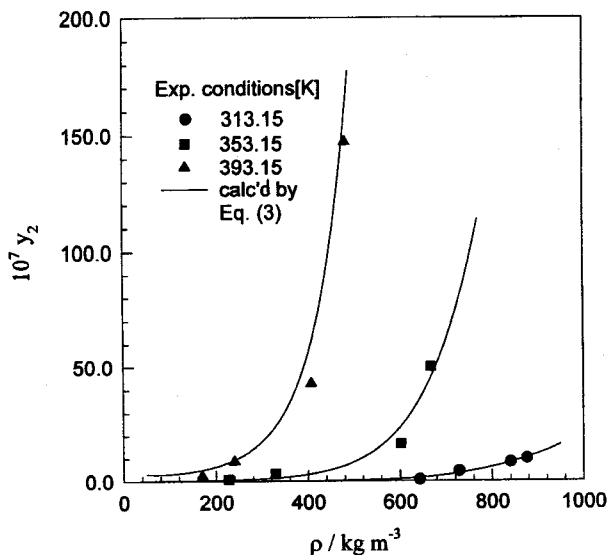


Fig. 4. Empirical solubility correlation by Eq. (3) for disperse red 1 in supercritical CO₂.

3. Modeling Solubility by NLF-EOS

In Table 5, the best-fitted temperature-dependent binary adjustable parameters of the NLF-EOS obtained from the experimental solubility data are summarized. Calculated solubili-

Table 5. Best-fit values of coefficients of binary interaction energy parameter, $\lambda_{12}(T)$ given by Eq. (6) for disperse dye/CO₂ systems

Mixtures	$10^3 \lambda_{12}^{(0)}$	$\lambda_{12}^{(1)}$
Disperse blue 14/CO ₂	2.836	-1.382
Disperse orange 11/CO ₂	3.524	-1.638
1-Methylamino-anthraquinone/CO ₂	2.836	-1.433
Disperse red 1/CO ₂	2.205	-1.157
Disperse yellow 7/CO ₂	2.745	-1.254

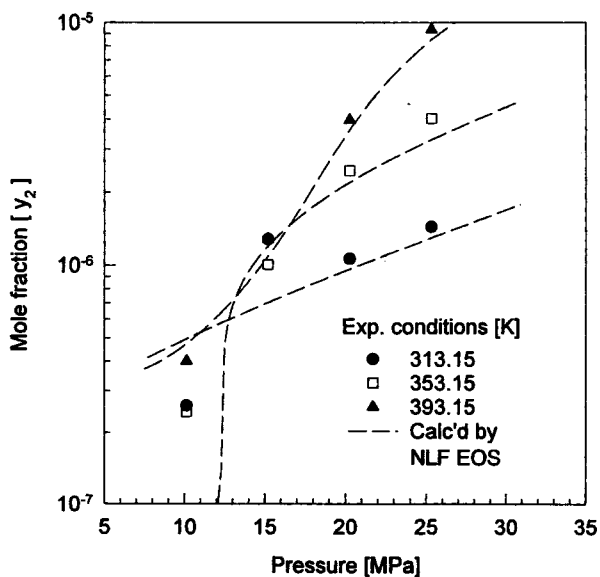


Fig. 5. Calculated solubility by the NLF-EOS for disperse blue 14 in supercritical CO₂.

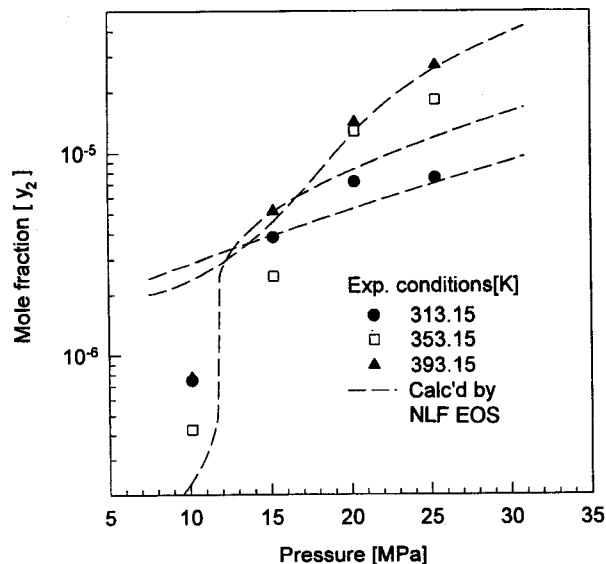


Fig. 6. Calculated solubility by the NLF EOS for disperse orange 11 in supercritical CO₂.

ty of disperse blue 14 in supercritical carbon dioxide at 313.15, 353.15 and 393.15 K is compared with experiment in Fig. 5. Except for the region in the vicinity of the critical point of carbon dioxide, the NLF-EOS correctly calculates the measured data well. The EOS also correctly predicts the crossover phenomenon of solubility around 15 MPa. In Fig. 6, the calculated solubility of disperse orange 11 in supercritical carbon dioxide by the EOS is shown. Except for the severe sensitivity of the model near the critical point of carbon dioxide, the EOS correctly fits the effect of supercritical pressure on the solubility of disperse orange 11. Similar correlation capability of the EOS is demonstrated in Fig. 7 on the solubility of disperse 1-methylaminoanthraquinone.

In Figs. 8 and 9, comparisons between the calculated and experimental solubility of disperse red 1 and disperse yellow

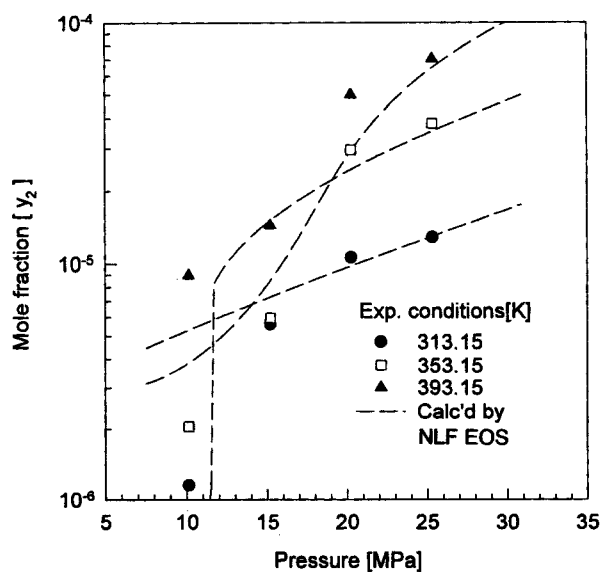


Fig. 7. Calculated solubility by the NLF EOS for disperse 1-methylamino-anthraquinone in supercritical CO₂.

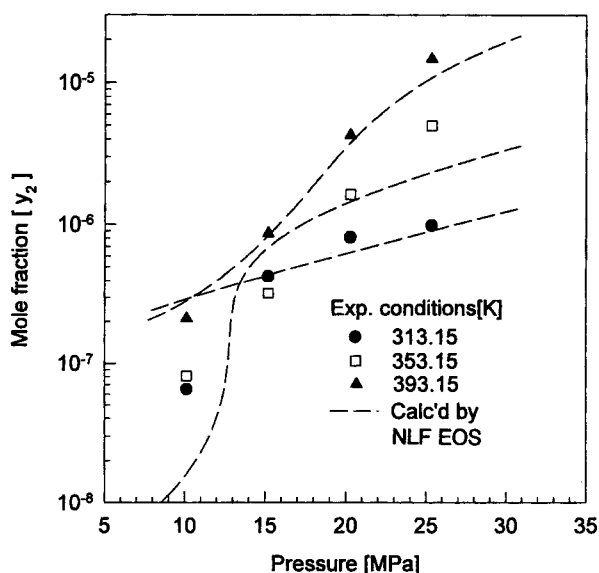


Fig. 8. Calculated solubility by the NLF EOS for disperse red 1 in supercritical CO₂.

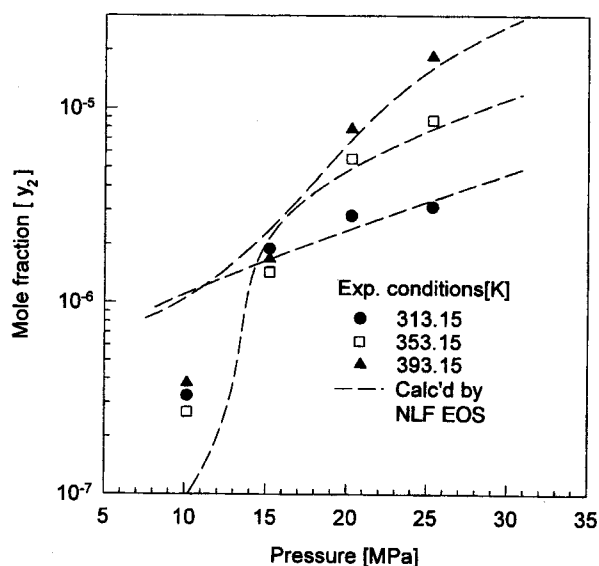


Fig. 9. Calculated solubility by the NLF EOS for disperse yellow 7 in supercritical CO₂.

7 in supercritical carbon dioxide are shown. The model fits the data reasonably well except in the near critical region of carbon dioxide. These inaccuracies of the fitting capability of the EOS in the critical region of carbon dioxide arise from the possible inaccurate estimation of the physical property constants of the dye substances and, thus, the possible uncertainty of the estimated pure EOS parameters given in Table 3. As long as further reliable pure properties of the dyes are available, the reliability of the EOS calculation can be enhanced.

CONCLUSION

The solubility of five disperse dyes (Celliton fast blue B, 1-amino-2-methylantraquinone, 1-methylaminoantraquinone,

disperse Red 1 and 4-[4-(phynylazo) phenylazo]-o-cresol) in supercritical carbon dioxide was measured in the ranges of temperatures from 313.15 to 393.15 K and pressures from 10 to 25 MPa. We found that the solubility in general was increasing with increasing temperature and pressure of CO₂.

To provide thermodynamic modeling information for SFD process design, an attempt was made to estimate the pure property constants of dyes. Also, an empirical model and the NLF-EOS are applied for the calculation of solubility of dyes in supercritical carbon dioxide. We concluded that both models calculated the solubility of dyes reasonably well.

ACKNOWLEDGEMENT

The authors are grateful to the Korea Science and Engineering Foundation for financial support. They also thank Dr. Min Jeong Noh for his valuable contribution.

REFERENCES

- Bartle, K. D., Clifford, A. A. and Jafar, S. A., "Solubilities of Solids and Liquids of Low Volatility in Supercritical Carbon Dioxide", *J. Phys. Chem. Ref. Data*, **20**, 713 (1991).
- Chiou, J. S., Barlow, J. W. and Paul, D. R., "Plasticization of Glassy Polymers by CO₂", *J. of Applied Polymer Sci.*, **30**, 2633 (1985).
- Chiou, J. S., Maeda, Y. and Paul, D. R., "Gas and Vapor in Polymers Just Below T_g", *J. Applied Polymer Sci.*, **30**, 4019 (1985).
- Chang, K. H., Bae, H. K. and Shim, J. J., "Dyeing of PET Textile Fibers and Films in Supercritical Carbon Dioxide", *Korean J. Chem. Eng.*, **13**(3), 310 (1996).
- Fleming, G. K. and Koros, W. J., "Dilation of Polymers by Sorption of Carbon Dioxide at Elevated Pressures", *Macromolecules*, **19**, 2285 (1986).
- Gebert, B., Saus, W., Knittel, D., Buschmann, H. J. and Schollmeyer, E., "Dyeing Natural Fibers with Disperse Dyes in Supercritical Carbon Dioxide", *Textile Res. J.*, **64**(7), 371 (1994).
- Knittel, D., Saus, W. and Schollmeyer, E., "Application of Supercritical Carbon Dioxide in Finishing Processes", *J. of the Textile Institute*, **84**, 534 (1993).
- Lyman, W. J., Reehl, W. F. and Rosenblatt, D. H., *HANDBOOK OF CHEMICAL PROPERTY ESTIMATION METHODS*, American Chemical Society, Washington, DC, 1990.
- Özcan, A. S., Clifford, A. A. and Bartle, K. D., "Solubility of Disperse Dyes in Supercritical Carbon Dioxide", *J. Chem. & Eng. Data*, **42**, 590 (1997).
- Reid, R. C., Prausnitz, J. M. and Poling, B. E., "The Properties of Gases & Liquids", 4th Ed., McGraw Hill, New York, 1987.
- Saus, W., Knittel, D. and Schollmeyer, E., "Dyeing of Textiles in Supercritical Carbon Dioxide", *Textile Res. J.*, **63**(3), 135 (1993).
- Swidersky, P., Haarhaus, U., Tuma, P. and Schneider, G. M., "High-pressure Investigations on the Solubility of Organic Dyes in Supercritical Gases by Vis/Nir Spectroscopy", *Korean J. Chem. Eng.*(Vol. 15, No. 1)

- Proc. of 3rd Int. Supercritical Fluids (Strasbourg, France, 17-19 October, 1994), 191 (1994).
- Timmermans, J., *Physico-Chemical Constants of Pure Organic Compounds*, Vol. 1 and Vol. 2, Elsevier Scientific Publishing Company, New York, 1950.
- You, S. S., Yoo, K.-P. and Lee, C. S., "An Approximate Non-random Lattice Theory of Fluids. General Derivation and Application to Pure Fluids", *Fluid Phase Equil.*, **93**, 193 (1994a).
- You, S. S., Yoo, K.-P. and Lee, C. S., "An Approximate Non-random Lattice Theory of Fluid Mixtures", *Fluid Phase Equil.*, **93**, 215 (1994b).
- You, S. S., Yoo, S. J., Yoo, K.-P. and Lee, C. S., "Multiphase Behavior and Critical Loci in Binary Mixtures Using A New Equation of State Based on the Nonrandom Lattice-Fluid Theory", *J. Supercritical Fluids*, **7**, 251 (1994c).